When a DNA triple helix melts: an analogue of the Efimov state

New Journal of Physics

When a DNA triple helix melts: an analogue of the Efimov state

Jaya Maji[1]**, Somendra M Bhattacharjee**[1,3]**, Flavio Seno**[2] **and Antonio Trovato**[2]

[1] Institute of Physics, Bhubaneswar 751005, India
[2] CNISM, Dipartimento di Fisica, Università di Padova, Via Marzolo 8, 35131 Padova, Italy
E-mail: jayamaji@iopb.res.in, somen@iopb.res.in, flavio.seno@pd.infn.it and antonio.trovato@pd.infn.it

Abstract. The base sequences of DNA contain the genetic code, and, to decode it, a double helical DNA has to be unzipped to reveal the bases. Recent studies have shown that a third strand can be used to identify the base sequences, not by opening the double helix but rather by forming a triple helix. It is predicted here that a three-strand DNA exhibits the unusual behaviour of the existence of a three-chain bound state in the absence of any two being bound. Such a state can occur at or above the duplex melting point. This phenomenon is analogous to the Efimov state in three-particle quantum mechanics. A scaling theory is used to justify the Efimov connection. Real space renormalization group (RG) and exact numerical calculations are used to validate the prediction of a biological Efimov effect.

[3] Author to whom any correspondence should be addressed.

IOP Institute of Physics ⏀ DEUTSCHE PHYSIKALISCHE GESELLSCHAFT

Contents

1. Introduction

Double helical DNA is common but, under certain circumstances, DNA can form a triple helix too. The 1957 discovery of a three-strand DNA remained a curiosity till the recognition in 1987 that a third strand of DNA can actually recognize the base sequence of the double helix even without opening it [1]–[3]. Owing to its enhanced stability, which can affect activities such as gene expression, DNA replication and others requiring DNA opening, the triple helix fostered new hopes in therapeutic applications [4]. To date, it has been possible to make and study triple helices *in vitro*, amidst high hopes of their relevance *in vivo* [5, 6]. At ambient temperatures, the double helix is formed with classical Watson–Crick base pairing, while the third strand forms non-classical Hoogsteen or (reverse Hoogsteen) base pairing with one of the other two. The triple helix can also be formed with DNA–RNA [7] and DNA–peptide nucleic acid (PNA), whose uncharged peptide backbone helps in the stabilization of the triplet structure [8, 9]. On a completely different front, in 1970 Efimov, in his studies on nucleons, showed an effect, now bearing his name, in three-body non-relativistic quantum mechanics, namely the possibility of a three-body bound state where none of the pairs is bound and the overall size of the bound state is much larger than the range of pair potentials [10]–[14]. One purpose of this paper is to wed these two disparate systems to show that an analogue of the quantum Efimov state is the triple helix *at or above* the double helix melting point.

The origin of the Efimov effect is the scale-free quantum fluctuation near the zero-energy threshold of two-body binding. The effective interaction that gives three-body binding does not depend on the detailed nature of the short-range interactions and is operative outside its range. Many years since its discovery, it is now seen in systems over various length scales ranging from nucleons (halo nucleus) to atomic physics and ultra-cold atoms under Feshbach resonance [15]–[17]. Triple stranded DNA near its melting point is shown to be a unique example from the domain of classical biology and might provide an affordable system for studying aspects of quantum Efimov physics.

There have been many physical, chemical and biological studies of triplex forming oligonucleotides (TFO) with applications in mind [18]. We take a thermodynamic point of view, where the long chain limit is taken to explore the nature of the phases and transitions of a triplex. The case of oligonucleotides can then be formulated by studying the finite-length effects on the transitions of the infinite chain system. Our focus in this paper is mainly on the infinite chain limit. A scaling approach is used here to see the origin of the Efimov effect via the development of a ubiquitous attractive $1/r^2$ interaction over a range beyond
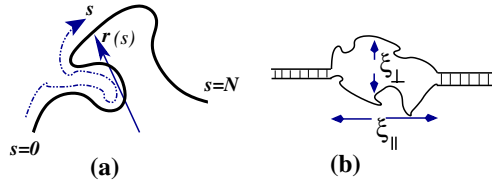
Figure 1. (a) A Gaussian chain or a random walker in three dimensions. An arbitrary point is specified by the contour length s and its position vector $\mathbf{r}(s)$, with the two ends at $s = 0$ and $s = N$. (b) A bubble on a two-chain system. The extent along the contour is $\xi_{\parallel}$ and the spatial extent is $\xi_{\perp}$. The ladder-like regions represent the bound states with base pairing between points with the same s.

the short range of the pair potential. The short range in the context of DNA is the hydrogen bond length or the base pair separation. The Efimov interaction requires a pairwise attraction at the critical threshold so a quantum system in $d \leqslant 2$ will not show this, because in these lower dimensions a bound state exists for any shallow potential. However, in a polymeric system, if a finite melting point can be induced, then the Efimov effect will be visible. In subsequent sections, we consider a few simplified polymer models to establish the Efimov effect in DNA. A renormalization group (RG) approach is used to show the Efimov-like three-chain phase in $d \geqslant 2$ models and a high-precision numerical approach is used for $1 + 1$-dimensional models. The phase diagram for the bubble-free three-chain fork model, with a first-order duplex melting, is discussed in appendix A. Some details of the RG calculation can be found in appendix B.

2. Scaling approach to the Efimov effect

Let us consider three Gaussian polymers interacting with one another through a DNA base pairing type short-range interaction. A monomer of a chain j ($j = 1, 2, 3$) is identified by a length variable s measured along the contour of the chain with $\mathbf{r}_j(s)$ as its position vector (see figure 1(a)). This and the models in the subsequent sections are coarse-grained models where what we call a monomer in fact represents several base pairs. The interaction involves monomers with the same s of different chains, so that the Hamiltonian for strands of length N ($N \to \infty$) can be written in a dimensionless form as [19]

$$\beta H = \int_0^N \mathrm{d}s \left[\sum_{j=1}^3 \frac{K_j}{2} \left(\frac{\partial \mathbf{r}_j(s)}{\partial s} \right)^2 + \sum_{k<l} V_{kl}(\mathbf{r}_k(s), \mathbf{r}_l(s)) \right], \tag{1}$$

where V_{kl} is the short-range attractive interaction representing the base pairing between chains k and l, and K_j is the elastic constant or flexibility of chain j; and $\beta = 1/k_B T$, with T being the temperature and k_B the Boltzmann constant. The first term on the rhs of equation (1) represents the elastic energy or the connectivity of the polymers. The partition function is given by

$$Z = \int \mathcal{D}R \exp(-\beta H), \tag{2}$$

where $\int \mathcal{D}R$ stands for the summation over all configurations or paths of the three chains with appropriate boundary conditions. We may choose $\mathbf{r}_j(0) = 0$ for all j, i.e. the three chains are tied at the origin at one end. The other ends may be free.
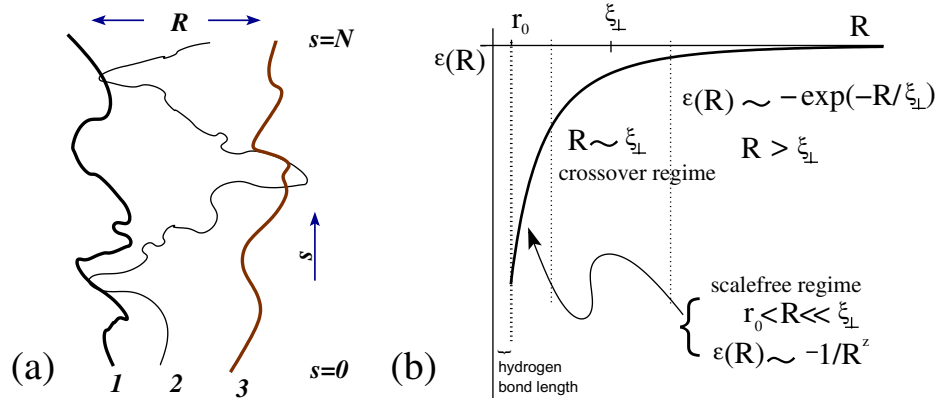
Figure 2. (a) Two non-interacting Gaussian chains 1 and 3 separated by a distance R. Each of these can pair with a flexible chain 2, denoted by the thin line. The polymers are shown with s as an axis. In the quantum correspondence, these polymers are the paths with s as the time-like axis. (b) The effective interaction $\epsilon(R)$ between 1 and 3. A triple chain bound state (Efimov effect) occurs in the region $r_0 < R \ll \xi_\perp$ and extends over the whole range for $\xi_\perp \to \infty$.

By treating the partition function as a path integral, the imaginary time transformation $s = \mathrm{i}t$ converts Z to a propagator in quantum mechanics for three particles with a pairwise interaction $V_{kl}(\mathbf{r}_k, \mathbf{r}_l)$, and the masses determined by K_j. With a short-range attractive potential of range r_0, there is a critical threshold of the potential in three dimensions for two particles to form a bound state, and for stronger potentials there will be a finite number of bound states. At the critical coupling, the two-particle system has a zero-energy bound state with infinite width of the eigenfunction or infinite scattering length [10]–[12].

The DNA–quantum correspondence relates the quantum critical threshold to the thermal melting of duplex DNA, a continuous transition in this model, with a diverging length scale [20, 21]. This scale can be associated with the transient bubbles that may form for temperatures just above the melting point T_c (analogous to the scattering length a of the quantum problem) or the fluctuation in size and shape of the bubbles below T_c (the width of the wave function in the quantum case). The bubbles can be characterized by two scales: $\xi_\perp$ for the spatial extent and

$$\xi_\parallel \sim \xi_\perp^z \tag{3}$$

for the length of the bubble (figure 1(b)), where $1/z$ is like a size exponent for polymers. For the quantum problem, with $\xi_\perp$ as the scattering length a, z corresponds to the dynamic exponent. The diffusive or Gaussian nature of the free chain for our case (or the quantum problem) implies

$$z = 2. \tag{4}$$

One can see this value of z from the scale invariance of the elastic energy term in equation (1). This term ensures the connectivity of a polymer and remains invariant under a scale transformation, $\mathbf{r} \to \lambda\mathbf{r}, s \to \lambda^z s$, with equation (4). A similar invariance argument yields equation (4) for the non-relativistic free particle Schrödinger equation.

Suppose that we have two non-interacting chains 1 and 3, both interacting with another one, chain 2. For simplicity, although not essential, we may take 1 and 3 as relatively stiffer compared to 2, and they are a distance R apart (see figure 2). Choose the pairwise interaction

between 1–2 and 2–3 or the temperature close to the critical threshold. In that case, if $\xi_\perp > R$, then in between two contacts with chain 1, chain 2 is expected to meet chain 3. The interaction is attractive. This exchange over a large length scale induces an attraction between 1 and 3 if chain 2 is integrated out from the partition function of equation (2). The effective interaction $\varepsilon(R)$ is the change in free energy $\Delta F/N$ because of the presence of a scale R, so it can be written as

$$\Delta F \sim -\frac{N}{\xi_\parallel}\, \mathcal{F}(R/\xi_\perp)\,, \tag{5}$$

where the first factor is the number of blobs and $\mathcal{F}(x)$ is a scaling function. For $\xi_\perp \to \infty$, equation (5) should be independent of it, requiring $\mathcal{F}(x) \sim x^{-z}$, as $x \to 0$, so that in this limit, by equation (4),

$$\varepsilon(R) \equiv \frac{\Delta F}{N} = -\frac{A}{R^z} = -\frac{A}{R^2} \quad (A \text{ is a constant}). \tag{6}$$

We see the emergence of a 'universal' $1/R^2$ interaction for a region $r_0 < R \ll \xi_\perp$, and this attractive long-range interaction can produce a bound state of size bigger than r_0. It should be noted here that, above the duplex melting point, there will be large bubbles, thanks to critical fluctuations, and so the attractive long-range interaction persists even above the melting point. This gives the possibility of a three-chain bound state where none is bound in the two-particle potential well.

In quantum language, the large fluctuation is the resonance, and the Efimov effect is due to the attraction produced by the multiple scattering of a light particle off the two heavier ones. This is one aspect of the Efimov effect. In an exact study using a separable potential (under the Born–Oppenheimer approximation), the effective interaction between 1 and 3 by the hopping of 2 was calculated [13]. The result of [13] can be recast in our scaling language (note that $\xi_\perp$ is the scattering length a) as

$$\varepsilon(R) = -\frac{1}{\xi_\perp^2}\, \frac{1}{\tilde{R}^z} \mathrm{f}(\tilde{R}), \quad \text{where } \tilde{R} = \frac{R}{\xi_\perp}, \tag{7}$$

and

$$\mathrm{f}(\tilde{R}) = \mathrm{e}^{-\tilde{R}}(2\tilde{R} + \mathrm{e}^{-\tilde{R}}), \tag{8}$$

corroborating the scaling hypothesis of equation (5). One sees a cross-over from $-1/R^2$ for $\tilde{R} \ll 1$ to the Yuakawa form $-\mathrm{e}^{-\tilde{R}}/\tilde{R}$ for $\tilde{R} \sim O(1)$. The scale-free interaction permeates the whole region for $\xi_\perp \to \infty$ at the critical or threshold value of the pair interaction. Figure 2(b) shows the nature of the effective interaction in the presence of a scale $\xi_\perp$. The Efimov interaction is beyond the hydrogen bond length of duplex DNA.

The Efimov interaction allows a three-chain bound state close to or just above the duplex melting point. The size of the bound state will necessarily be much larger than the hydrogen bond strength. The fact that one sees Efimov states, although finite in number, for large but finite $\xi_\perp$ (equation (8)) indicates that the triple helix DNA may also show an Efimov analogue bound state even above the duplex melting temperature. This also means that the melting temperature is higher for a triplex than for a duplex. The minimal model in equation (1) has a continuous transition. If other interactions not in equation (1) drive the transition first order, the length scale $\xi_\perp$ will be non-diverging. However, if the transition is weakly first order, $\xi_\perp$ may be large enough to accommodate the intermediate scale-free region shown in figure 2(b), allowing a bound state. Hence, in a weak first-order transition with large $\xi_\perp$, one would still see the Efimov-like bound
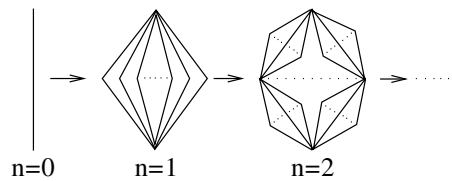
Figure 3. Recursive construction of the hierarchical lattice used for the real space RG. At every stage, each line is replaced by a diamond of $2b$ lines.

state. The case of a strong first-order transition is dealt with in appendix A, where it is shown that the effect is absent if the bubbles are fully suppressed.

The second aspect of the Efimov effect is that, at the critical point, there is an infinite sequence of bound states in a geometric form $E_n = E_0(e^{-2\pi/s_0})^n$, where s_0 is a system-specific number (e.g. for three identical bosons, $s_0 = 1.00624$). The energy scale E_0 is also system parameter dependent. The above analysis is done with the ground-state dominance assumption that is justifiable for $N \to \infty$. The polymer partition function of equation (2) for finite N is given by the Efimov energies as

$$Z \sim C_1 \exp(-E_0 N) + C_2 \exp(-E_1 N) + \cdots, \tag{9}$$

where the temperature has been absorbed in the 'energies'. The terms beyond the ground state can be ignored if

$$N \gg 1/|E_1 - E_0| \sim \frac{1}{|E_0(1 - e^{-2\pi/s_0})|}. \tag{10}$$

This is the length requirement for the triple DNA to show the Efimov-like state.

The prediction of a large girth triplex close to (and even above) the duplex DNA melting point awaits experimental tests.

3. Efimov-like phase in $d \geqslant 2$

In order to justify the prediction of the scaling theory in a systematic way, we adopt an RG [22] approach for $d > 2$. In the RG approach, the effects of interaction are probed by summing over the configurations at a smaller scale (in the partition function) and redefining the effective interaction on a larger scale. For a bound state, we should see an effective interaction among the chains, irrespective of the scale of coarse-graining. In contrast, for an unbound state, locally bound monomers lose their importance as we sum over configurations, and therefore the effective interaction will vanish as the probing length scale increases. These effects are expressed by the RG flow equations or recursion relations, as flows of the interactions with length scale. A two-body bound state should therefore be possible if the two-body interaction does not vanish. In the same spirit, a three-body bound state will occur if a three-body interaction becomes operative, even if there is none to start with. We express these RG relations in an exact form on specially constructed hierarchical lattices with discrete scaling symmetry and tunable dimensionality.

Let us consider three directed polymers, which are doing random walk from bottom to top on a hierarchical lattice, constructed recursively with a motif of $2b$ bonds, as shown in figure 3. The branching factor b determines the effective dimension (d) of the hierarchical lattice as
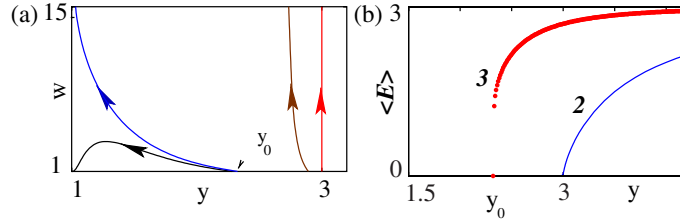
Figure 4. (a) RG flow diagram in the y–w-plane for the symmetric case $y_{12} = y_{23} = y_{13}$, all starting with $w = 1$. Here $b = 4$. The flow of w goes to ∞ if the starting $y > y_0 = 2.32402\ldots$, otherwise it goes to 1 (high-temperature fixed point). The trajectories with starting $y < y_0$ end at $w = y = 1$. (b) Average energy per monomer versus temperature from direct computation (chain length $= 2^{25}$). For two chains (marked 2), the average energy undergoes a continuous transition at $y = y_c$, while the average energy for three chains (marked 3) shows a jump at $y = y_0$. The region from y_0 to y_c is the Efimov-like three-chain bound state.

$d = \ln 2b / \ln 2$. There are attractive potentials $-\epsilon_{ij}$ and $-\epsilon_{ijk}$ ($\epsilon_{ij}, \epsilon_{ijk} > 0$) if a single bond is shared by two and three polymers, respectively. Although $\epsilon_{123} = 0$, still it will be needed for the RG transformation to probe the three-body bound state and is generated by renormalization.

The configurations of the two-chain system can be classified as two independent chains or inherently two-chain configurations. The corresponding recursion relation for the two-chain Boltzmann factors $y_{ij} = \exp(\beta \epsilon_{ij})$ is given by [22],

$$y'_{ij} = \frac{b - 1 + y_{ij}^2}{b}. \tag{11}$$

Similarly, the three-chain configurations can be classified as (i) three independent chains, (ii) a combination of a double and a single chain or (iii) inherently three-chain configurations, i.e. three-chains sharing the same bond. By a decimation of the $2b$-bond motif, the recursion relation for the three chain-Boltzmann factor $w = \exp(\beta \epsilon_{123})$ is given by

$$w' = \frac{(b-1)(b-2) + (b-1)\sum_{i<j} y_{ij}^2 + w^2 \prod_{i<j} y_{ij}^2}{b^2 \prod_{i<j} y'_{ij}}, \tag{12}$$

where y' and w' denote the renormalized values.

In the following discussion, we choose the initial value $w = 1$. The three fixed points of y_{ij} correspond to (i) $y^* = \infty$ (zero temperature, pure bound state), (ii) $y^* = 1$ (infinite temperature, no two-body interaction) and (iii) $y^* = (b - 1)$ (two-chain unstable critical point).

In case there is no pairwise bound state or no pair interaction, w has two fixed points 1 and $b^2 - 1$. The stable fixed point 1 describes the high-temperature fixed point or absence of three-body interaction, and the unstable fixed point $b^2 - 1$ describes the critical state produced by a pure three-body interaction. The flow going to infinity is indicative of the three-chain bound state, formed by the three-body force, a case not of interest here.

In case all pairs are in the critical state so far as the two-body interaction is concerned ($y_{ij}^* = b - 1$), there is no real fixed point for w. The renormalization flow takes w to infinity, as shown in figure 4(a). The three chains then form a bound state at the two-body critical point. For
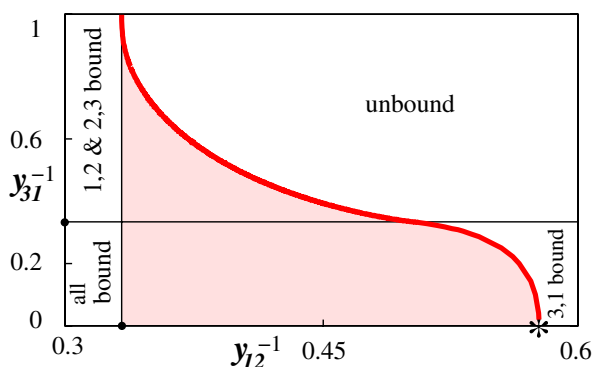
Figure 5. Phase diagram: y_{31}^{-1} versus y_{12}^{-1} ($y_{12} = y_{23}$), for $b = 4$. The duplex melting point at $y_c^{\{ij\}} = b - 1$ is indicated by the horizontal and vertical lines. Three chains are bound in the shaded region with the thick curve representing the three-chain bound–unbound transition. Above the horizontal line at $y_{31} = b - 1$ in the shaded region, a triplex state exists even though no two should be bound. The bound states in other regions are as indicated. The star at $y_{12}^{-1} = 1/\sqrt{b-1}$ is the melting of chain 2 and composite 1, 3.

temperatures above the duplex melting, i.e. with initial values $y = y_{12} = y_{23} = y_{31} < b - 1$, the triplex will be in the denatured state if the flow goes to $y = 1$, $w = 1$. For example, for $b = 4$, the three-chain melting is at $y = 2.32402\ldots$, which is less than the duplex melting point $y_c = 3$. Further confirmation of this triplex melting comes from an exact numerical calculation of the average energy by iterating the partition functions and their derivatives for large lattices. This is shown in figure 4(b). With $y \equiv y_{12} = y_{23} = y_{31}$, as in figure 4(a), the two-strand system melts through a second-order transition at $y = y_c$ (energy going continuously to 0), whereas the three-strand system undergoes a first-order transition at a temperature $y = y_0 < y_c$ (energy showing a discontinuity; see appendix B for details). The region between $y = y_0$ and $y = y_c$ is the region of a triple-strand bound state when there should not be any duplex.

The phase diagram in the plane of y_{13}^{-1} versus y_{12}^{-1} with $y_{12} = y_{23}$, $w = 1$ is shown in figure 5. For $y_{13}^{-1} = 0$, chains 1 and 3 are bound forever and therefore chain 2 melts off at $y_{12} = \sqrt{b-1}$. This point is indicated by a star in figure 5. Within the triangular-shaded region bounded by $y_{13}^{-1} = 1/(b-1)$, $y_{12}^{-1} = 1/(b-1)$ and the curved line separating the unbound state, we have a triplex phase without pairing of any two—the desired Efimov effect.

4. Numerical simulation in $d = 1 + 1$

After arguing for the existence of an Efimov bound state for triple DNA helices through the DNA–quantum correspondence and the scaling argument, and after observing the effect on a hierarchical diamond lattice, in this section we produce clear numerical evidence that the effect is present in a Euclidean lattice even in $1 + 1$ dimensions.

Directed polymers in such a dimensionality are amenable to exact solutions in the thermodynamic limit of infinite chain length or for extremely accurate numerical simulations since their interchain contacts are guaranteed to occur between monomers (see figure 6) with the same index, as for DNA. For such reasons, they played an important role in clarifying melting, cold unzipping and overstretching properties of duplex DNA [23]–[25], and for the same reasons they turn out to be the most convenient models in which to test numerically the
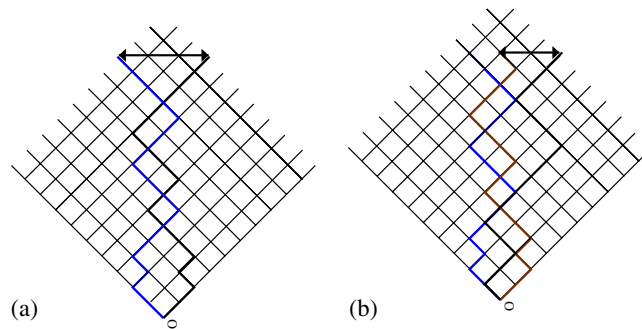
Figure 6. (a) Graphical representation of directed two-strand DNA in 1+1 dimensions. The two strands start from the same origin and are directed along the direction (1, 1). The walks can cross each other. Each bubble opening is weighted with a factor σ, each interaction (overlap of the two chains) with a weight y. The weight of this conformation is therefore $\sigma^5 y^5$. Note that each interaction corresponds to sites with the same index. (b) The three chain-models. A factor σ is given to each bubble opening among all possible pairs of polymers. For model A, the weight of this configuration is $\sigma^{11} y^{12}$ (see text). For model B, where the interaction is only between the red and the blue chain, and the red and the brown chain, the weight is $\sigma^{11} y^9$. The black arrows, in both figures, indicate the end-to-end distance r_N used to estimate the melting transition.

existence of the Efimov effect that at higher dimensions might be obscured by the noise of numerical simulations.

Here, we consider duplex DNA formed by directed polymers that can cross each other (see figure 6). Such models do not show any melting transition at finite temperatures in $1 + 1$ dimensions. In the quantum mechanics analogy, the dimension along which the polymers are directed plays the role of time: then it is well known that any short-range potential, no matter how weak, will produce a bound state for $d \leqslant 2$.

Nevertheless, keeping the notation $y = \exp(\beta\epsilon)$ for the Boltzmann factor associated with base pair interaction, if we introduce a fugacity σ for each bubble formed in the model between the two DNA strands, it is possible to demonstrate that the melting transition $y_c(\sigma)$ decreases from $y_c(1) = 1$ (i.e. $(T = \infty)$) for $\sigma = 1$ to $y_c(0) = 2$ for $\sigma = 0$ (i.e. for the fork model in which bubbles are suppressed). See appendix A for the phase diagram of the fork model.

In order to generalize the model for three chains (see figure 6), we associate the fugacity σ with each bubble opening between all possible pairs of chains. As regards the base pair interactions, we consider two options:

- In model A, we assign a Boltzmann factor y for all two-chain interactions, but, in the case when all three chains come together, we assign an interaction factor y^2 instead of y^3.

- In model B, we assign a Boltzmann factor y for each interaction between chain 1 and chain 2, and between chain 2 and chain 3, but we do not consider any interaction between chain 1 and chain 3.

In both cases, the melting temperatures of the three- and two-chain systems coincide at $\sigma = 0$, when bubbles are forbidden. The existence for a given σ of a three-chain bound state at a $y < y_c(\sigma)$, for $0 < \sigma < 1$, should be definitive proof of the Efimov effect for models of triplex DNA.
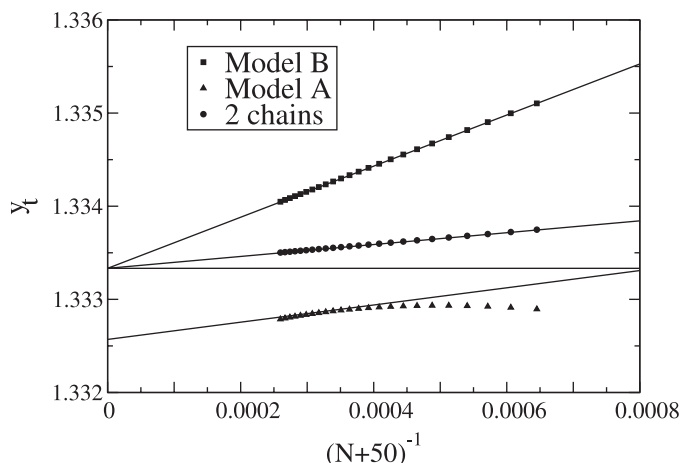
Figure 7. For models A and B described in the text and for a two-strand model, we estimate the denaturation transition by looking, in the three cases, at the crossing y_t of the curves $\xi_N(y)$ and ξ_{N+100}, where N is ranging from 1500 to 3900 in steps of 100. These crossing points are plotted as a function of $1/(N+50)$. The case $\sigma = 0.5$ is considered. The horizontal continuous line represents the exact melting value $y_t = 4/3$ of the duplex model. Linear extrapolation curves are also shown. Their intercepts with the y-axis are 1.3333 ± 0.0001 for model B, 1.3333 ± 0.0001 for the two chains and 1.3326 ± 0.0001 for model A. These results definitely show that model B has the same melting transition as the duplex model, whereas model A melts at a higher temperature (Efimov effect).

It is known [20] that in 1+1 dimensions, if a polymer is confined between two lines or two polymers, there is a repulsive entropic force of a similar $1/r^2$ potential. In our model B, chain 2 is the only one that can mediate interaction between 1 and 3, because the latter two chains do not interact, and, for chain 2 to do so, it becomes effectively, although not strictly, confined between chains 1 and 3. In such a situation, the steric repulsion and the induced attractive interaction between 1 and 3 tend to cancel each other [26]. This weakens the possibility of the Efimov effect in model B but not in the case of model A. The non-existence of the Efimov effect in model B would therefore be further proof that our analysis is correctly taking care of all possible interactions of the models.

The three-chain models cannot be solved exactly but they can be numerically studied with impressive precision through transfer matrix techniques. We worked at $\sigma = 0.5$. For this value, the melting transition occurs at $y_m \equiv y_c(0.5) = 4/3$. The existence of the melting transition can be seen by looking at the rescaled average distance $\xi_N \equiv r_N/(N^{1/2})$ between the free extrema of an arbitrary pair of the three chains at a length N. By using standard finite size scaling techniques, in order to pinpoint the transition temperature, we computed the intersection between these curves. The resulting numbers are presented in figure 7. In the figure, besides the data for model A and model B, we also show the data for the exactly solvable two-chain model in order to evaluate the degree of convergence of the simulations.

Beyond any possible numerical uncertainty, model B, as we argued, already does not show any Efimov effect, while model A exhibits the Efimov effect. Although narrow, there exists a temperature interval for model A in which three chains are bound, whereas two are not.

5. Conclusion

We have presented a scaling argument to show the possibility of a three-strand DNA bound state in conditions where duplex DNA would be in the denatured state. This is a biological analogue of the nuclear or cold atom Efimov effect. The scaling argument is further confirmed by RG and exact numerical results from various model systems in different dimensions.

We end with a few comments. To mimic reality, the minimal model considered here may be supplemented with additional terms like excluded volume effects, whose influence on the phenomenon needs separate analysis. However, if experiments can be done in theta conditions for the strands, then the excluded volume effects can be ignored or minimized, and our results would be applicable. It may be noted that enzymatic activities are hypothesized to involve local covalent or hydrogen bonds and contacts. For DNA, one requires denaturation of strands (melting in some form) locally. In these lock and key mechanisms, the issue of non-specific long-range bonds is generally not considered. Therefore, the existence of a bound state involving two otherwise denatured strands of DNA due to the presence of a third strand, with overall separation much larger than the hydrogen bond length, would have important implications for biological processes. Nonetheless, we anticipate new experiments to look for signatures of our proposed Efimov-DNA.

Appendix A. Phase diagram in the absence of loops (Fork model)

In order to get the thermodynamic phase diagram, we consider a simplified model of three chains without bubbles by generalizing the double chain Y-model studied in the context of the melting and unzipping transition of a duplex [23, 24].

Consider three chains on a standard square lattice, stretched along one diagonal direction (directed polymers). The polymers interact with pairwise contact interactions $-\epsilon_{ij}$ between chains i and j. The monomers are indexed from one end $s = 0$. By construction, the interchain interaction is between monomers with the same index, as is required for DNA. There is an additional constraint that an unbound configuration of two chains cannot be followed by a bound stretch along the increasing s direction. This avoids loops on the chains but allows opening of the DNA. This is the Y-model. For this model, every open chain has an entropy $k_B \ln \mu$ per monomer ($\mu = 2$ steps per bond) and the same entropy for any bound polymer (duplex or triplex). With this entropy and the additive energy, the free energies per monomer for various possible phases can be written. These are (with $k_B = 1$)

$$f_b = -(\epsilon_{12} + \epsilon_{23} + \epsilon_{31}) - T \ln \mu \quad \text{(all bound)}, \tag{A.1a}$$

$$f_u = -3T \ln \mu \quad \text{(all unbound)}, \tag{A.1b}$$

$$f_{ij,k} = -\epsilon_{ij} - 2T \ln \mu \quad (ij \text{ bound}, k \text{ free}). \tag{A.1c}$$

The two-chain melting transition is at $T_c^{\{jk\}} = \epsilon_{jk}/(\ln \mu)$.

The phase transition lines in this Y-model are all first-order lines whose slopes can be determined by a Clausius–Clapeyron argument. Let us take a line of coexistence between two types of phases A and B in a phase diagram of 'intensive' variables X_1 and X_2. Let the conjugate extensive variables be $\rho_i = \partial F/\partial X_i$, with F being the appropriate free energy. At a given point
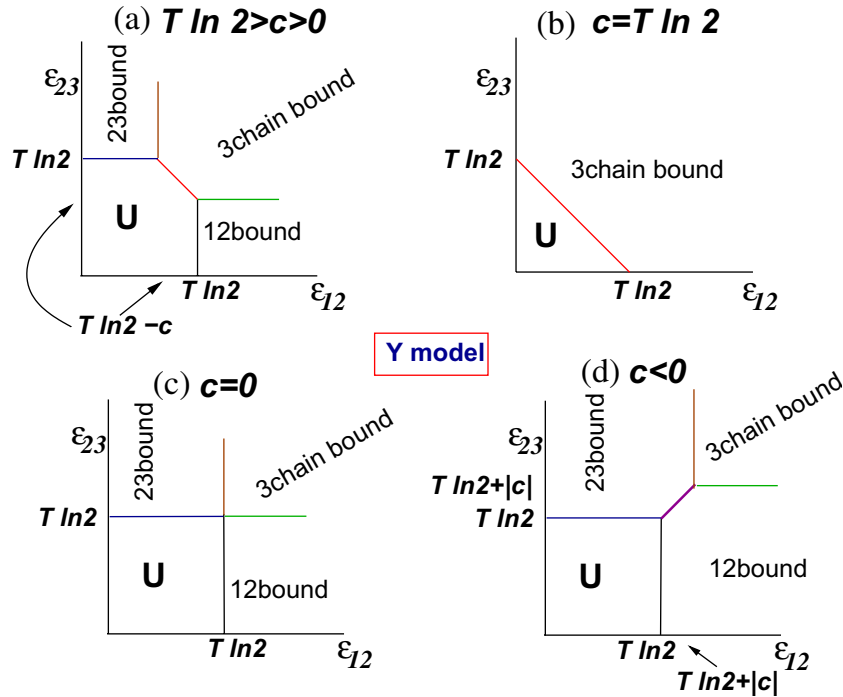
Figure A.1. Phase diagrams for the three-chain Y-model. Here, $c = \epsilon_{31}$. $c < 0$ corresponds to repulsive interaction. 'U' represents the unbound state.

on the coexistence curve, ρ_i would show a discontinuity, taking values ρ_i^A and ρ_i^B in the two phases. Then the slope of the line is given by

$$\frac{\partial X_2}{\partial X_1} = -\frac{\rho_1^A - \rho_1^B}{\rho_2^A - \rho_2^B}. \tag{A.2}$$

In our case, $X_1 \equiv \beta\epsilon_{12}$, $X_2 \equiv \beta\epsilon_{23}$ and so the derivative of the free energy gives the associated number of contacts. Consequently, the slope is related to $\Delta n_{12}/\Delta n_{23}$. Now, in this all-or-none Y-model, these differences in the fraction of contacts in the two phases are either 1 or 0. Therefore, the slopes can, in general, be 0 or ∞. The special case is line $X_1 = X_2$. By symmetry, here on this line $\Delta n_{12} = \pm\Delta n_{23}$ and the slope should be ± 1.

   If one chain melts away, i.e. a triplex breaks into a duplex and a free chain, then $T_{b\to 12}, T_{b\to 23} < T_{b\to u}$. These conditions follow from the stability of the phases as given by the free energies. We therefore have two inequalities: for the $\{12, 3\}$-state to occur, $\epsilon_{12} > \epsilon_{23} + \epsilon_{31}$, and for state $\{23, 1\}$ to occur, $\epsilon_{23} > \epsilon_{12} + \epsilon_{31}$. For easy display, we represent the three-dimensional phase (3D) diagram in slices of the ϵ_{12}–ϵ_{23} plane for given values of $c = \epsilon_{13}$ and T. Figure A.1 shows four possible situations for different values of ϵ_{31} and T. In these figures, $c = T \ln 2$ is special because of melting of the 1–3 pair. There is a region in figure A.1(a) where one sees a three-chain bound state in a range of temperatures where none of the pairs would be bound. Despite the similarity with the Efimov effect, the bound state is purely from the pairwise binding and in that sense it is not a true representative of the effect[4]. The figures show that at or above the melting temperature of the 1–3 pair or if chains 1 and 3 are non-interacting ($c = 0$, figure A.1(c)), the three-chain bound phase may melt via a duplex or directly to the unbound state. Direct melting without an intervening duplex phase is not possible if $c < 0$ (figure A.1(d)).

---

[4] Surface adsorption can lead to renaturation of two strands. See, for example, [27].
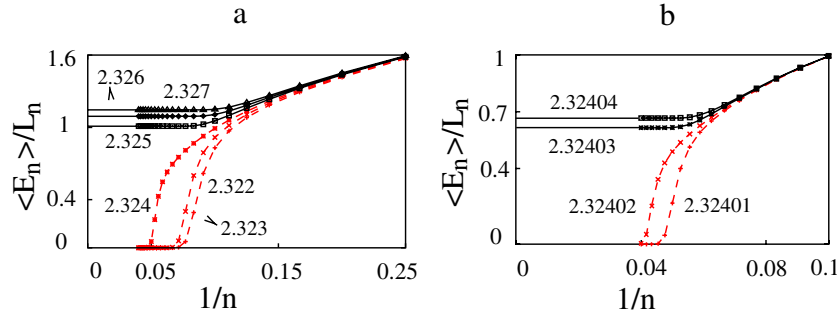
Figure B.1. Plots of E_n/L_n versus $1/n$, with E_n being the three-chain average energy and n the generation number. We went up to $n = 25$ for which the length of each polymer is $L_n = 2^{25}$. In (a) we show for $y = 2.322 + 0.001 * n$, $n = 0$–5, while a finer grid result is shown in (b) with $y = 2.324\,00 + 0.000\,01 * n$, $n = 1$–4. The lines show the extrapolations to $n \to \infty$. The discontinuity at the transition is visible.

Experimental phase diagrams for the triple helix are generally created with temperature and salt concentration as the two variables. For a given concentration, the variation in the temperature would follow a particular trajectory in the 3D thermodynamic phase space, and the possible phases one would see are determined by the intersection of that curve with the phase boundaries.

Appendix B. Evidence of a first-order transition for the triplex

We present numerical evidence that there is a discontinuity in the three-chain average energy, as shown in figure 4(b).

The exact value of E_n at the nth generation is computed by using MATHEMATICA with infinite precision by iterating the two- and three-chain partition functions and their derivatives. The length of the polymers at the nth generation is $L_n = 2^n$, so that the thermodynamic limit of energy per monomer E_n/L_n can be obtained by extrapolation to $1/n \to 0$. If C_n, Z_n and Q_n are the nth generation partition functions for single, double and triple chain systems, then these obey the recursion relations [22],

$$C_n = bC_{n-1}^2, \tag{B.1}$$

$$Z_n = b(b-1)C_{n-1}^4 + bZ_{n-1}^2, \tag{B.2}$$

$$Q_n = b(b-1)(b-2)C_{n-1}^6 + b(b-1)C_{n-1}^2 \sum_{\substack{i,j=1 \\ i<j}}^{3} Z(ij)_{n-1}^2 + bQ_{n-1}^2, \tag{B.3}$$

where the arguments of Z_{n-1} in equation (B.3) refer to the two chains involved. The initial conditions are

$$C_0 = 1, \quad Z_0 = y, \quad Q_0 = y^3.$$

The relations for the derivatives can be derived from equations (B.1)–(B.3).

Figure B.1 shows the extrapolation in the range of $y = 2.323$–2.327, which brackets the transition in the range $(2.324, 2.325)$. The discontinuity survives even on a finer scale in figure B.1(b), which gives y_0 in the range $(2.324\,02, 2.324\,03)$ consistent with the RG result of figure 4.

References

[1] Felsenfeld G, Davies D R and Rich A 1957 *J. Am. Chem. Soc.* **79** 2023
[2] Moser H E and Dervan P B 1987 *Science* **238** 645
[3] Le Doan T *et al* 1987 *Nucleic Acids Res.* **15** 7749
[4] Jain A *et al* 2008 *Biocheimie* **90** 1117
     Duca M *et al* 2008 *Nucleic Acids Res.* **36** 5123
[5] Frank-Kamenetskii M D and Mirkin S M 1995 *Annu. Rev. Biochem.* **64** 65
[6] Soifer V and Potaman V N 1996 *Triple-Helical Nucleic Acids* (New York: Springer)
[7] Roberts R W and Crothers D M 1992 *Science* **258** 1463
[8] Nielsen P E 1995 *Annu. Rev. Biophys. Biomol. Struct.* **24** 167
[9] Betts L *et al* 1995 *Science* **270** 1838
[10] Efimov V 1970 *Phys. Lett.* B **33** 563
[11] Efimov V 1970 *Yad. Fiz.* **12** 1080
      Efimov V 1971 *Sov. J. Nucl. Phys.* **12** 589 (Engl. Transl.)
[12] Efimov V 1979 *Sov. J. Nucl. Phys.* **29** 546
[13] Fonseca A C, Redish E F and Shanley P E 1979 *Nucl. Phys.* A **320** 273
[14] Braaten E and Hammer H W 2006 *Phys. Rep.* **428** 259
[15] Zaccanti M *et al* 2009 *Nat. Phys.* **5** 586
[16] Kraemer T *et al* 2006 *Nature* **440** 315
[17] Fedorov D V, Jensen A S and Riisager K 1994 *Phys. Rev. Lett.* **73** 2817
[18] Plum G E 1997 *Biopolymers* **44** 241
[19] Bhattacharjee S M 2000 *J. Phys. A: Math. Gen.* **33** L423
[20] Fisher M E 1984 *J. Stat. Phys.* **34** 667
[21] Gothoh O 1983 *Adv. Biophys.* **16** 1
[22] Mukherji S and Bhattacharjee S M 1995 *Phys. Rev. E* **52** 1930
[23] Marenduzzo D, Trovato A and Maritan A 2001 *Phys. Rev. E* **64** 031901
[24] Marenduzzo D, Bhattacharjee S M, Maritan A, Orlandini E and Seno F 2002 *Phys. Rev. Lett.* **88** 028102
[25] Marenduzzo D, Orlandini E, Seno F and Trovato A 2010 *Phys. Rev. E* **81** 051926
[26] Brak R *et al* 2007 *J. Phys. A: Math. Theor.* **40** 4415
[27] Allahverdyan A E *et al* 2006 *Phys. Rev. Lett.* **96** 098302
      Allahverdyan A E *et al* 2009 *Phys. Rev. E* **79** 031903